Chemical Science

ROYAL SOCIETY OF CHEMISTRY

EDGE ARTICLE

View Article Online
View Journal | View Issue

Cite this: *Chem. Sci.*, 2025, **16**, 21379

All publication charges for this article have been paid for by the Royal Society of Chemistry

Unprecedented allosteric inhibition of *E. coli* malate dehydrogenase by silver(I) from atomic resolution analysis

Haibo Wang,[a] Minji Wang,[b] Xinming Yang,[a] Aixin Yan,[b] Quan Hao,[c] Hongyan Li[a] and Hongzhe Sun*[a]

Received 12th July 2025
Accepted 19th September 2025

DOI: 10.1039/d5sc05183e

rsc.li/chemical-science

Metal ions may functionally inhibit metalloproteins *via* either replacement of intact metal cofactors or binding to allosteric sites *via* metalloallostery. Despite extensive studies, until now, it has not been fully understood how silver inhibits its authentic protein targets, particularly at the atomic level, largely owing to the lack of knowledge on the authentic protein targets of silver as well as the limited structures available. Herein we show that malate dehydrogenase (MDH) serves as a vital target of antimicrobial Ag^+ against *E. coli*. Ag^+ binds MDH at multiple sites and inhibits its activity *via* a non-competitive mechanism. Importantly, we successfully captured the Ag^+-mediated "open-to-closed" conformational change of the active-site of MDH by X-ray crystallography. Combined with the enzyme kinetics and mutagenesis data, we unambiguously unveil that the allosteric inhibition of MDH by Ag^+ is attributable to its binding to the cysteine residue (Cys251), consequently leading to the closure of the active-site loop of MDH, which disrupts the substrate and coenzyme binding, and ultimately inhibiting the activity of MDH. Our studies provide the first structural glimpse of an unprecedented allosteric inhibition of authentic target enzymes by silver. These findings not only enhance our understanding of the mechanism underlying silver inhibition of its protein targets at the atomic level, but also offer a novel allosteric targeting site in MDH for the design of new antibiotics.

Introduction

Metal ions, *e.g.*, silver (Ag^+),[1–7] bismuth (Bi^{3+}),[8–11] and gallium (Ga^{3+}),[12–15] have been widely used as antimicrobial agents for decades.[3,16–18] In particular, silver and silver nanoparticles (AgNPs) are the most widely used antibacterial agents in healthcare and the food industry,[1–4,19,20] whereas their molecular targets have remained largely concealed throughout history.[3,21–26] It is commonly believed that silver (Ag^+) toxicity is due to the binding of silver to enzymes *via* the thiolate or thioester of cysteine or methionine residues, resulting in subsequent substitution of the cognate ions in the catalytic sites of metalloenzymes.[2,3,27] Given that metal ions could regulate metalloprotein functions *via* binding to allosteric sites through metalloallostery,[28] it remains elusive whether silver could also inhibit enzymes *via* allosteric sites, which has been recognized as an emerging approach for drug discovery and development.[29,30] Owing to the fact that Ag^+ is isoelectronic to Cu^+, most studies feature binding of silver to copper transporters[31–36] and transcriptional regulators,[37,38] and the active site of copper enzymes,[39] leading to disruption of copper homeostasis.[40,41] However, the binding of silver to its authentic protein targets and the bio-coordination chemistry of silver remain poorly understood due to the limited silver-binding protein structures determined, a consequence of the technical challenges involved.[6,42] This scarcity has hindered a comprehensive investigation into the targeting sites and residues of silver, as well as its inhibitory mode of action, particularly at the atomic level.

Malate dehydrogenase (MDH) is a core metabolic enzyme that catalyzes the reversible oxidation of malate to oxaloacetate with the concomitant reduction of NADH.[43–58] It has been proposed to be a drug target due to its crucial role in cellular metabolism and its involvement in various diseases.[59] Using a home-made platform, we have identified *E. coli* malate dehydrogenase (*Ec*MDH) as one of the silver-binding proteins in the bacteria.[60,61] *Ec*MDH is an enzyme that has no metal ion cofactors in central carbon metabolism, and possesses three cysteine residues and several methionine–histidine pairs. All these cysteine sites are neither adjacent to the active site nor directly involved in the catalytic process. These properties render *Ec*MDH an exceptional model to investigate silver and its protein targets at the molecular level, *e.g.*, targeting sites or residues of silver ions in proteins, the mechanism underlying silver inhibition of enzymes, and the coordination geometry of

[a]*Department of Chemistry and HKU-CAS Joint Laboratory of Metallomics on Health and Environment, The University of Hong Kong, Pokfulam Road, Hong Kong, P. R. China. E-mail: hsun@hku.hk*

[b]*School of Biological Sciences, The University of Hong Kong, Pokfulam Road, Hong Kong, P. R. China*

[c]*School of Biomedical Sciences, The University of Hong Kong, Sassoon Road, Pokfulam, Hong Kong, P. R. China*

silver ions and its relationship with the inhibition mode. Such studies will yield new information on the biological and medicinal chemistry of Ag^+, and uncover new targeting sites for development of new antibacterial agents.

Herein, we show that MDH serves as a vital target of Ag^+ in cells for its antibacterial activity against *E. coli*. Our systemic biochemical characterization demonstrates that Ag^+ binds to MDH at multiple sites and inhibits MDH in a non-competitive mode. Importantly, we captured the Ag^+-mediated "open" to "closed" conformational change of the MDH active-site by X-ray crystallography. Binding of Ag^+ to the Cys251 residue at the allosteric site led to the closure of the active site by the movement of a loop (residues 79–91), resulting in an unprecedented allosteric inhibition of MDH by Ag^+.

Results and discussion

MDH serves as a vital protein target of antibacterial Ag^+ against *E. coli*

We identified 34 silver-bound proteins in *E. coli via* a home-made platform.[60] We delineated that Ag^+ primarily damages multiple enzymes in the TCA cycle, leading to the stalling of the oxidative branch of the TCA cycle and an adaptive metabolic divergence to the reductive glyoxylate shunt, subsequently damaging the adaptive glyoxylate shunt, and leading to the death of the bacterium.[60] Among the five identified silver-binding proteins in the TCA cycle and glyoxylate shunt, *i.e.*, isocitrate dehydrogenase (IDH), succinyl-CoA synthetase subunit alpha (SucD), malate dehydrogenase (MDH), malate lyase (AceA), and malate synthase A (AceB), MDH is the only enzyme involved in both pathways (Fig. 1A), indicative of its importance in mediating the antibacterial activity of Ag^+ against *E. coli*. MDH. The enzyme has aroused great interest due to its vital role as a key enzyme in the central oxidative pathway and other metabolic activities, including aspartate biosynthesis, the malate–aspartate shuttle, gluconeogenesis, and lipogenesis.[43–58] In view of the multiple roles of MDH in various biological processes, we hypothesize that MDH may serve as an important target of Ag^+ against *E. coli*.

To verify whether MDH is an authentic Ag^+-binding protein, we extracted cytosolic proteins from both wild-type (WT) *E. coli* MG1655 and gene knockout strain Δ*mdh* after treatment with $AgNO_3$ and compared the GE-ICP-MS profiles of Ag^+-binding proteins in the molecular weight (MW) window at around 32

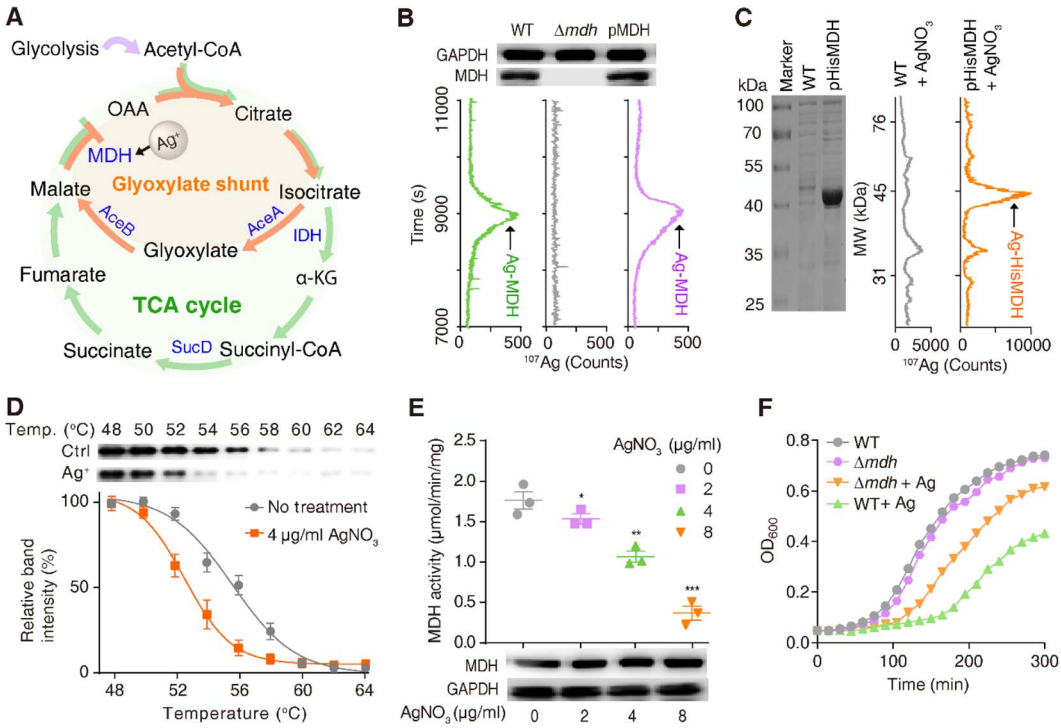

Fig. 1 Malate dehydrogenase (MDH) as a vital protein target of antimicrobial silver ions against *E. coli*. (A) Scheme of TCA cycle (green) and glyoxylate shunt (orange) in *E. coli*. The identified silver-binding proteins in our previous study are shown in blue. (B) GE-ICP-MS electropherograms (^{107}Ag) for WT *E. coli*, Δ*mdh* mutant, and Δ*mdh* strain transformed with the plasmid (*p*MDH) that expresses MDH. Soluble proteins were extracted from bacterial cells (OD_{600} of 0.3) after treatment with 4 μg ml^{-1} $AgNO_3$ for 1 h and further analyzed by LC-GE-ICP-MS. ^{107}Ag profiles of proteins with isoelectric points in the range of 5 to 6 are shown. The presence or absence of MDH was verified by western blotting. (C) GE-ICP-MS profiles of the soluble proteins extracted from WT *E. coli* and pHis$_6$MDH strain (His$_6$MDH being overexpressed by IPTG induction). (D) Cellular thermal shift assay (CETSA) of WT *E. coli* with or without treatment of 4 μg ml^{-1} $AgNO_3$ ($n = 3$, ±SEM). The intracellular MDH protein in the soluble fractions was quantified by western-blotting. The band intensities at different temperatures are normalized to that of 48 °C. (E) The activity of MDH in *E. coli* after treatment with 0, 2, 4, and 8 μg ml^{-1} $AgNO_3$ ($n = 3$, ±SEM). The abundance of MDH under different conditions was quantified by western blotting with GAPDH as internal standard. (F) Growth of WT *E. coli* and Δ*mdh* variant with or without treatment of 4 μg ml^{-1} $AgNO_3$ ($n = 3$, ±SEM). All experiments were performed in triplicate. One representative of three replicates is shown (B, C, and F). Results are shown as mean ± SEM (D and E). *$P < 0.05$, **$P < 0.01$ and ***$P < 0.001$.

kDa. The results showed that the peaks corresponding to Ag^+-MDH at around 32 kDa disappeared in the Δ*mdh* strain, but reappeared when the plasmid containing *mdh* was transformed into a Δ*mdh* mutant (Fig. 1B). The presence or absence of MDH in the extracted cell lysates was confirmed by western blotting (Fig. 1B). We further examined the GE-ICP-MS profile of cell lysate from *E. coli* with His_6-MDH being overexpressed by IPTG induction. A distinct and intense peak of ^{107}Ag at around 45 kDa (the observable MW of His_6-MDH is around 45 kDa) was observed compared to that of WT *E. coli* (Fig. 1C), indicating that Ag^+ binds to the overexpressed His_6-MDH. These data collectively demonstrate that MDH is an authentic Ag^+-binding protein in *E. coli*.

We next examined whether Ag^+ binds to MDH *in cellulo* by a cellular thermal shift assay (CETSA).[62,63] *E. coli* cells after treatment with 4 μg ml^{-1} (IC_{50} value) $AgNO_3$ for 1 h in Luria–Bertani (LB) medium were harvested and subjected to the CETSA analysis pursuant to the standard protocol.[62,63] As shown in Fig. 1D, the treatment of Ag^+ yielded a shift in the apparent aggregation temperature (T_{agg}) of intracellular MDH from 55.6 °C to 52.6 °C, confirming that Ag^+ binds to MDH and destabilizes the thermal stability of MDH *in cellulo*.

We further studied the effect of Ag^+ binding on the function of MDH *in cellulo* by extracting the lysate of *E. coli* cells after treatment with various concentrations of Ag^+ and measured the MDH activity. The expression level of MDH was quantified by western-blotting using GAPDH as an internal standard to rule out the alteration of MDH activity induced by a distinct abundance of MDH. After normalizing MDH abundance, the activity of MDH was found to decrease significantly from 1.8 U mg^{-1} (nontreated) to 1.5, 1.1 and 0.37 U mg^{-1} in the cell lysates of *E. coli* upon treatment with 2, 4 and 8 μg ml^{-1} of $AgNO_3$ respectively (Fig. 1E), demonstrating that binding of Ag^+ to MDH inhibits its activity without affecting its expression level *in cellulo*.

We also explored whether the Ag^+-mediated inhibition of MDH activity could contribute to the antibacterial activity of Ag^+ against *E. coli*. We examined the growth of the wild-type (WT) and Δ*mdh E. coli* strains upon treatment with 4 μg ml^{-1} $AgNO_3$. As shown in Fig. 1F, the WT and Δ*mdh* strains exhibited nearly identical growth curves in the absence of Ag^+. In contrast, addition of Ag^+ resulted in distinct growth curves for the two strains, with WT culture displaying a much longer lag phase and slower growth than the Δ*mdh* strain, suggesting that the deletion of *mdh* contributes to the silver tolerance of *E. coli*. The fact that Δ*mdh* mutant culture is less sensitive to Ag^+ suggests that targeting of MDH by Ag^+ contributes to its antibacterial activity against *E. coli*, consistent with a recent report.[23] Taken together, we demonstrate that Ag^+ binds to MDH and inhibits MDH activity *in cellulo*, which could be attributed to its antimicrobial activity against *E. coli*.

Ag^+ binds to MDH cysteine residues at the non-active site

We next studied how Ag^+ binds to MDH *in vitro*; we overexpressed and purified the MDH protein. The identity of MDH was characterized by MALDI-TOF MS (Table S1). Purified MDH

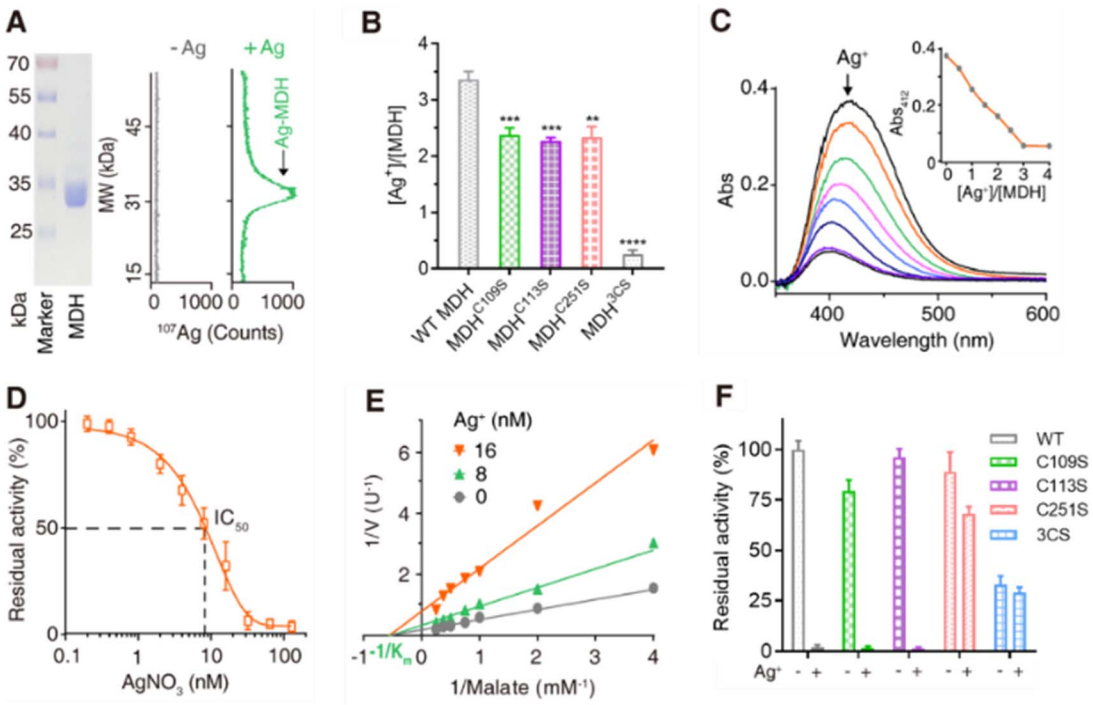

Fig. 2 Ag^+ ions bind to MDH mainly *via* three cysteine sites and inhibit MDH in a non-competitive mode. (A) SDS-PAGE of purified MDH and GE-ICP-MS electropherograms (^{107}Ag) of MDH with or without treatment of Ag^+ ($n = 3$). (B) MALDI-TOF mass spectra of apo-MDH and MDH after incubation with 4 and 8 eq. of Ag^+ ($n = 3$). (C) Free thiol contents in MDH measured by Ellman's assay ($n = 3$). The absorbance at 412 nm is plotted against Ag^+/MDH ratios. (D) Dose dependent inhibition of MDH by Ag^+ ($n = 3$, ±SEM). (E) Lineweaver Burk plots ($n = 3$). (F) Normalized residual activity of WT MDH and MDH variants ($n = 3$, ±SEM). One representative of three replicates is shown (A and C).

was incubated with 4 molar equivalents (eq.) of Ag^+ and then subjected to GE-ICP-MS analysis.[61] A single peak of ^{107}Ag at a MW of *ca.* 32 kDa corresponding to a monomer of Ag-bound MDH was observed (Fig. 2A), indicative of the binding of Ag^+ to MDH *in vitro*. Binding of Ag^+ to MDH (monomer) was further examined by ICP-MS. The binding ratio of Ag^+ to the WT MDH was measured to be 3.36 ± 0.14 by quantifying the amounts of the protein and the metal by the BCA assay and ICP-MS respectively (Fig. 2B).

Given that silver is highly thiophilic, we then examined whether the three cysteine residues (Cys109, Cys113, and Cys251) of MDH are involved in Ag^+ binding. The contents of free thiols of MDH pre-incubated with different molar ratios of Ag^+ were measured by Ellman's assay. As shown in Fig. 2C, Ag^+ treatment led to loss of the same amount of free thiol with 3 eq. Ag^+ completely depleting the free thiols in MDH. We subsequently mutated the three Cys residues to Ser individually, and the Ellman's assay showed that 2 eq. of Ag^+ could completely deplete the free thiols in the three single Cys variants (Fig. S1A–C). We then prepared the double Cys mutants, and found that incubation of 1 molar eq. of Ag^+ with the double Cys mutants could deplete the free thiols (Fig. S1D–F). Consistent with the Ellman's assay, the ICP-MS results showed that MDH^{C109S}, MDH^{C113S} and MDH^{C251S} bind one Ag^+ ion less per monomer than WT MDH, whereas the triple Cys mutant only binds 0.26 ± 0.07 Ag^+ ion per monomer, indicating the fourth weak binding site of Met227/His177. These data collectively demonstrate that the three cysteines are involved in Ag^+ binding. Our combined data from ICP-MS and Ellman's assay show that Ag^+ ions bind to MDH mainly *via* cysteine residues and each cysteine site binds one Ag^+ ion.

We further investigated Ag^+ inhibition of MDH *in vitro* by measuring the activity of MDH upon incubation with various amounts of Ag^+ ions. A dose-dependent inhibition of enzymatic activity of purified MDH by Ag^+ with an IC_{50} of 8.5 ± 1.3 nM was observed (Fig. 2D). We then examined the effects of Ag^+ at different concentrations on the enzyme kinetics of MDH with the malate varying from 0.13 to 4 mM without changing the NAD^+ level. The apparent V_{max} decreased from 5.3 to 1.3 U mg^{-1} with the increase of Ag^+ from 0 to 16 nM, whereas the K_m values of Ag^+-inactivated MDH for malate were similar to that of the native enzyme (Fig. 2E). The corresponding Lineweaver Burk plots indicate that Ag^+ exerts the inhibitory effect *via* a non-competitive inhibition mode.

Given that Ag^+ exhibits strong inhibition towards MDH with 90% of the MDH activity being inhibited by 16 nM of Ag^+, such a strong inhibition is unlikely to be achieved through binding of Ag^+ to the weakest site,[42] although it is the active site. Moreover, enzyme kinetics show a non-competitive inhibition of MDH activity by silver ions; we therefore hypothesize that the inhibition of MDH by silver ions is largely due to its binding to the three cysteine sites at the non-active site. To further investigate the targeting site of Ag^+ in MDH, we compared the enzyme activity of WT MDH and MDH mutants with or without treatment of Ag^+. Similar to the WT MDH, the activity of MDH^{C109S} and MDH^{C113S} could be completely inhibited by 16 nM Ag^+, while only *ca.* 20% and 5% decreases in the activity of MDH^{C251S} and MDH^{3CS} were observed respectively (Fig. 2F). The results demonstrate that the mutation of Cys251 to Ser renders the enzyme much less sensitive to silver, indicating that Ag^+ inhibition on MDH might be attributed to its binding to Cys251 at the non-active site.

Our combined data from enzyme kinetics and site mutagenesis showed that silver ions inhibit MDH activity in a non-competitive mechanism with its binding to the non-active Cys251 site being a major contributor to the inhibition. Thus, it is possible that the binding of silver ions to Cys251 site induces a conformational change of MDH and subsequently inactivates the enzyme through an allosteric regulation.

X-ray crystallography reveals allosteric inhibition of MDH by silver

We further explored the mechanism underlying Ag^+ inhibition of MDH through binding to Cys251 at the atomic level. We obtained Ag-bound MDH ($Ag\text{-}MDH^{WT}$) through co-crystalizing MDH with Ag^+ and solved its structure at the resolution of 2.22 Å (Fig. 3A, S2, and Table S4). In the $Ag\text{-}MDH^{WT}$ structure, two Ag^+ ions were observed with one at the Cys113 site and another one at the Cys251 site. Ag^+ was identified from the significantly positive peaks ($\geq 18\sigma$) in the m*Fo*-D*Fc* (difference Fourier) map (Table S5). At the Cys251 site, the Ag^+ ion coordinated with the thiolate of Cys251 and a water molecule in a quasi-linear geometry (O–Ag–S 143.0°) (Fig. 3B, Tables S6 and S7). At the Cys113 site, the Ag^+ ion binds to the thiolate group of Cys113 and, surprisingly, to the NH_2 group of a Tris molecule, with a nearly linear coordination geometry as well (N–Ag–S 156.1°) (Fig. 3C, Tables S6 and S7). The hydroxyl group of the Tris ligand was further stabilized by the side chains of two adjacent residues (Tris/O1···Lys142/Nζ 2.4 Å, Tris/O3···Asp71/Oδ1 2.6 Å). Superimposition of $Ag\text{-}MDH^{WT}$ with Ag-bound MDH^{WT} obtained by soaking showed that the two silver ions in $Ag\text{-}MDH^{WT}$ overlap with one of the two silvers at Cys251 (near Glu250) and Cys113 (near Lys142) sites in Ag-MDH (soaking) (Fig. S3).

Based on previously reported *E. coli* MDH structures, the active-site loop comprising residues 79–91 can be either in an open or a closed conformation.[48,64,65] In the presence of a malate analogue (*e.g.*, citrate and sulfate), the active-site loop closes over the substrate binding cavity,[48,64,65] otherwise, the two monomers (one per dimer) adopt an open conformation with one of the monomers' loops comprising residues 79–91 shifting

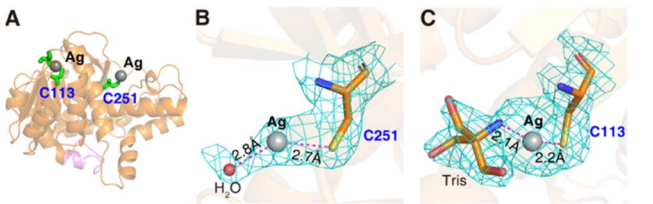

Fig. 3 Crystallographic analysis of Ag^+ binding to MDH. (A) Overall structure of $Ag\text{-}MDH^{WT}$. The coordination geometry of Ag^+ at Cys251 (B) and Cys113 (C) sites. Silver, water and 2*mFo-DFc* map are shown as grey spheres, red spheres, and cyan mesh (contoured at 1.0σ), respectively.

position to expose the substrate-binding pocket with the other being disordered.[48] Similarly, the active-site loops of the apo-MDH structures at 1.54 Å we determined were disordered in all monomers.

Unexpectedly, in the Ag-MDH^{WT} structure, we observed the electron density for the full length MDH including the active-site loop. Superimposition of 298 C_α atoms (excluding residues of 79–91) of Ag-MDH^{WT} with those MDH structures with the open (PDB ID: 1IE3) and closed (PDB ID: 1IB6) active-site loop conformations gave rise to RMSDs of 0.386 and 0.338 Å respectively (Fig. S4A). Significant conformational changes of the active-site loop were noted. In the Ag-MDH^{WT} structure, the loop not only bent over the substrate and NAD^+ binding sites compared to that in an open conformation (PDB ID: 1IE3) (Fig. 4A), but also closed even more "completely" than the closed state (PDB ID: 1IB6) (Fig. 4B, S4B and C). More specifically, the C_α atom of Ag-MDH^{WT} Gly84 (located in the middle of the loop) shifted by 10.8 and 5.7 Å compared to the MDH structures with the active-site loop open (PDB ID: 1IE3) and closed (PDB ID: 1IB6) respectively (Fig. 4B). In addition, superimposition of Ag-MDH^{WT} and MDH with the closed conformation (PDBID: 1IB6) showed that the residues of Ala80 and Arg81 of Ag-MDH ^{WT} occupy the position of the ribose ring and the nicotinamide of the NAD^+ as well as one of the substrate analogues SO_4^{2-} in 1IB6 (Fig. 4C). These observations collectively demonstrate that Ag^+ induced closure of the active-site pocket of MDH hinders the binding of the substrate and cofactor NAD^+, thereby resulting in allosteric inhibition of MDH.

We next investigated which silver binding site is responsible for the conformational change. Given that mutation of Cys251 to Ser led to the enzyme being less sensitive to silver (*vide supra*), we therefore speculate that the binding of Ag^+ to Cys251 might be correlated with the movement of the active-site loop. To confirm this, we obtained the Ag-bound MDH^{C251S} crystals (Ag-MDH^{C251S}) under the identical crystallization conditions to Ag-MDH^{WT} and solved its structure by X-ray crystallography at the resolution of 1.56 Å (Fig. S5A). In Ag-MDH^{C251S}, one Ag^+ ion coordinated to the thiolate group of Cys113 and H_2O, which is further stabilized by the main-chain oxygen of Lys111 ($H_2O341\cdots$Lys111/O 3.0 Å) (Fig. S5B, Tables S6 and S7) while no Ag^+ at the Ser251 site was observed. Superimposition of 296 C_α atoms (excluding residues 79–91) of Ag-MDH^{C251S} and Ag-MDH^{WT} shows an RMSD of 0.299 Å, indicative of no significant conformational change between Ag-MDH^{C251S} and Ag-MDH ^{WT} for 296 C_α atoms. However, different from Ag-MDH^{WT}, the active-site loop of Ag-MDH^{C251S} is disordered with no electron density being observed in all of the four chains in the unit-cell (Fig. S5A), indicating that the active site loop of MDH is in the open conformation, and Ag^+ binding to Cys251 induces the movement of the active-site loop and subsequent closure of the active-site cavity, which consequently disrupts the substrate and cofactor binding.

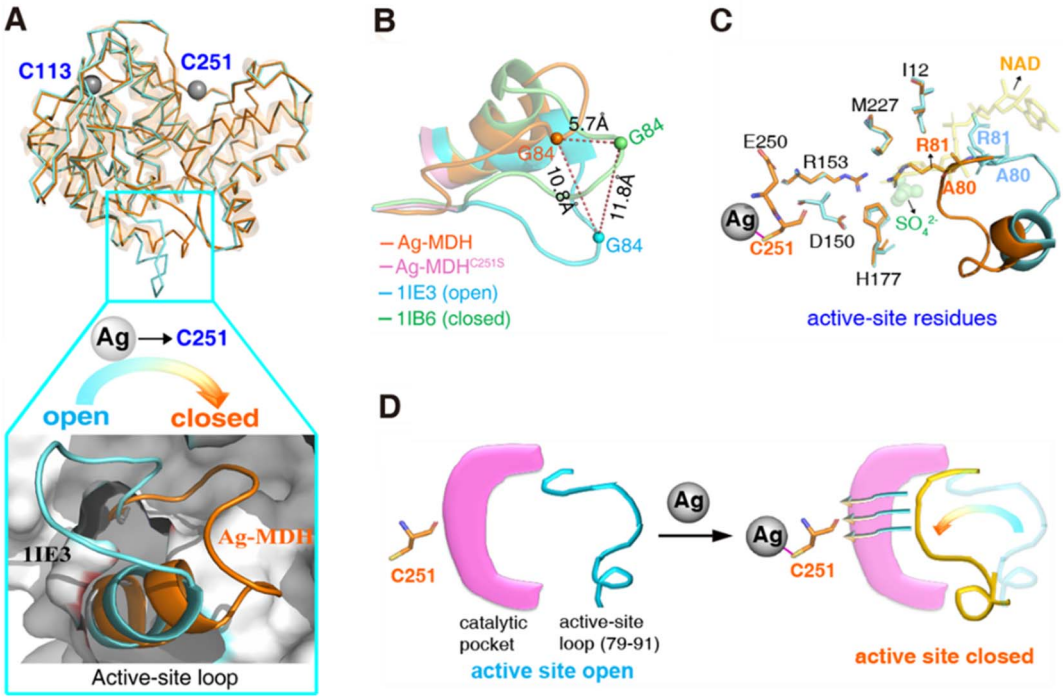

Fig. 4 Crystallographic analysis reveals that binding of Ag^+ to Cys251 at the allosteric site induces the closure of the MDH active site. (A) Overlay of the active-site loop of apo-MDH (PDB ID: 1IE3, in cyan) and Ag-MDH ^{WT} (in orange). The catalytic pocket is shown on the surface. (B) The distance shifted between Ag-MDH ^{WT} and active-site closed 1IB6 or opened 1IE3. The movements of residue Gly84 located in the middle of the loop are shown. (C) Comparison of the residues in the catalytic pocket of MDH. NAD^+ and SO_4^{2-} are from MDH with the active-site closed (PDB ID: 1IB6). (D) The scheme shows how Ag^+ induces closure of the MDH active site. Silver, water and 2*mFo-DFc* map are shown as grey spheres, red spheres, and cyan mesh (contoured at 1.0σ), respectively.

Conclusions

In summary, we demonstrate that Ag^+ binds and inhibits *Ec*MDH *in cellulo*, which contributes to the antibacterial activity of Ag^+ against *E. coli*. We show by systemic biochemical characterization that Ag^+ ions bind *Ec*MDH at multiple sites and inhibit MDH in a non-competitive mode. Significantly, we successfully captured the Ag^+-mediated "open-to-closed" conformational change of MDH active-site (Fig. 4D), leading to the allosteric inhibition of MDH upon binding of Ag^+ to the Cys251 residue. This appears to be the first structural glimpse of allosteric enzyme inhibition by Ag^+, representing a new paradigm for Ag^+ inhibition of its authentic protein targets. We also demonstrated that Ag^+ targets Cys149 and His176 at the active site of GAPDH (an essential enzyme in the glycolysis pathway without using a metal ion as the cofactor), leading to abolishment of its enzymatic activity *via* a mix-type inhibition.[66] These findings challenge the widely accepted hypothesis that silver toxicity is largely attributed to its ability to substitute the cognate ions in the catalytic sites of metalloenzymes. The inhibitory mechanism provides novel insights into the mode of action of antimicrobial silver and in turn, offers a new strategy for the design of new antibiotics *via* inhibition of key enzymes at the allosteric site. Our study may serve as a starting point for further drug development by targeting MDH, which serves as an important target for anticancer and antibacterial drug discovery.[49] Moreover, our strategy to identify hidden allosteric sites at the atomic level offers an exemplified approach to target the "untargetable" sites of a protein.

Author contributions

H. W., H. L. and H. S. conceived the idea and designed the study, analysed the results and wrote the manuscript. H. W. and X. Y. performed the study of protein purification. H. W. performed most of the biological characterization, including GE-ICP-MS, MALDI-TOF MS, Ellman's assay, and enzyme activity test. X. Y. and H. W. performed the ITC study. H. W. performed the CETSA study. H. W. designed and performed the protein crystallization. M. W. and H. W. analysed the crystal data.

Conflicts of interest

The authors declare no conflict of interest.

Data availability

Partial data have been uploaded as part of the SI. The coordinates and structure factors of apo-MDH^{WT}, Ag- MDH^{WT}, and Ag-MDH^{C251S} are deposited at the Protein Data Bank (wwPDB) with accession codes 6KA1, 6KA0, and 9WXS respectively. Supplementary information is available. See DOI: https://doi.org/10.1039/d5sc05183e.

Acknowledgements

We gratefully acknowledge the Research Grants Council of Hong Kong (SRFS2122-7S04, 17308921) and The University of Hong Kong (Norman Cecilia Yip Foundation and URC) as well as a Hong Kong PhD Fellowship (HKPF) for H. W. We thank the Center for Genomic Sciences, Li Ka Shing Faculty of Medicine for the mass spectrometry facilities. The crystal diffraction data were collected at Shanghai Synchrotron Radiation Facility (SSRF), the Chinese Academy of Sciences. We thank the staff at BL17U1 beamline of SSRF for their generous help.

Notes and references

1 S. Chernousova and M. Epple, *Angew. Chem., Int. Ed.*, 2013, **52**, 1636–1653.
2 S. Eckhardt, P. S. Brunetto, J. Gagnon, M. Priebe, B. Giese and K. M. Fromm, *Chem. Rev.*, 2013, **113**, 4708–4754.
3 J. A. Lemire, J. J. Harrison and R. J. Turner, *Nat. Rev. Microbiol.*, 2013, **11**, 371–384.
4 J.-Y. Maillard and P. Hartemann, *Crit. Rev. Microbiol.*, 2013, **39**, 373–383.
5 K. Zheng, M. I. Setyawati, D. T. Leong and J. Xie, *Coord. Chem. Rev.*, 2018, **357**, 1–17.
6 H. Wang, M. Wang, X. Xu, P. Gao, Z. Xu, Q. Zhang, H. Li, A. Yan, R. Y. Kao and H. Sun, *Nat. Commun.*, 2021, **12**, 3331.
7 A. Frei, A. D. Verderosa, A. G. Elliott, J. Zuegg and M. A. T. Blaskovich, *Nat. Rev. Chem.*, 2023, **7**, 202–224.
8 H. Li, R. Wang and H. Sun, *Acc. Chem. Res.*, 2019, **52**, 216–227.
9 X. Yang, M. Koohi-Moghadam, R. Wang, Y.-Y. Chang, P. C. Y. Woo, J. Wang, H. Li and H. Sun, *PLoS Biol.*, 2018, **16**, e2003887.
10 R. Wang, T.-P. Lai, P. Gao, H. Zhang, P.-L. Ho, P. C.-Y. Woo, G. Ma, R. Y.-T. Kao, H. Li and H. Sun, *Nat. Commun.*, 2018, **9**, 439.
11 Y. Xia, X. Wei, P. Gao, C. Wang, A. de Jong, J. H. K. Chen, M. J. Rodriguez-Sanchez, A. Rodriguez-Nogales, P. Diez-Echave, J. Galvez, F. Garcia, W. Wu, R. Y. Kao, H. Li, R. Cebrian, O. P. Kuipers and H. Sun, *Nat. Microbiol.*, 2024, **9**, 2600–2613.
12 Y. Wang, B. Han, Y. Xie, H. Wang, R. Wang, W. Xia, H. Li and H. Sun, *Chem. Sci.*, 2019, **10**, 6099–6106.
13 S. R. Choi, B. E. Britigan and P. Narayanasamy, *ACS Infect. Dis.*, 2019, **5**, 1559–1569.
14 C. H. Goss, Y. Kaneko, L. Khuu, G. D. Anderson, S. Ravishankar, M. L. Aitken, N. Lechtzin, G. Zhou, D. M. Czyz, K. McLean, O. Olakanmi, H. A. Shuman, M. Teresi, E. Wilhelm, E. Caldwell, S. J. Salipante, D. B. Hornick, R. J. Siehnel, L. Becker, B. E. Britigan and P. K. Singh, *Sci. Transl. Med.*, 2018, **10**, eaat7520.
15 C. Wang, Y. Xia, R. Wang, J. Li, C. L. Chan, R. Y. Kao, P. H. Toy, P. L. Ho, H. Li and H. Sun, *Nat. Commun.*, 2023, **14**, 5311.
16 N. P. E. Barry and P. J. Sadler, *Chem. Commun.*, 2013, **49**, 5106–5131.
17 H. Li and H. Sun, *Curr. Opin. Chem. Biol.*, 2012, **16**, 74–83.
18 C. Wang, X. Wei, L. Zhong, C. L. Chan, H. Li and H. Sun, *J. Am. Chem. Soc.*, 2025, **147**, 12361–12380.

19 J. W. Alexander, *Surg. Infect.*, 2009, **10**, 289–292.
20 M. J. Hajipour, K. M. Fromm, A. Akbar Ashkarran, D. Jimenez de Aberasturi, I. R. d. Larramendi, T. Rojo, V. Serpooshan, W. J. Parak and M. Mahmoudi, *Trends Biotechnol.*, 2012, **30**, 499–511.
21 K. D. Mjos and C. Orvig, *Chem. Rev.*, 2014, **114**, 4540–4563.
22 C.-N. Lok, C.-M. Ho, R. Chen, Q.-Y. He, W.-Y. Yu, H. Sun, P. K.-H. Tam, J.-F. Chiu and C.-M. Che, *J. Proteome Res.*, 2006, **5**, 916–924.
23 N. Gugala, J. Lemire, K. Chatfield-Reed, Y. Yan, G. Chua and R. J. Turner, *Genes*, 2018, **9**, 344.
24 W. K. Jung, H. C. Koo, K. W. Kim, S. Shin, S. H. Kim and Y. H. Park, *Appl. Environ. Microbiol.*, 2008, **74**, 2171–2178.
25 W.-R. Li, X.-B. Xie, Q.-S. Shi, H.-Y. Zeng, Y.-S. Ou-Yang and Y.-B. Chen, *Appl. Microbiol. Biotechnol.*, 2010, **85**, 1115–1122.
26 Q. L. Feng, J. Wu, G. Q. Chen, F. Z. Cui, T. N. Kim, J. O. Kim and J. Biomed, *Mater. Rep.*, 2000, **52**, 662–668.
27 J. L. Clement and P. S. Jarrett, *Met.-Based Drugs*, 1994, **1**, 467–482.
28 V. N. Pham and C. J. Chang, *Angew. Chem., Int. Ed.*, 2023, **62**, e202213644.
29 S. Y. Lu, Q. C. Shen and J. Zhang, *Acc. Chem. Res.*, 2019, **52**, 492–500.
30 A. Christopoulos, *Nat. Rev. Drug Discovery*, 2002, **1**, 198–210.
31 F. Long, C.-C. Su, M. T. Zimmermann, S. E. Boyken, K. R. Rajashankar, R. L. Jernigan and E. W. Yu, *Nature*, 2010, **467**, 484–488.
32 X. Du, H. Li, X. Wang, Q. Liu, J. Ni and H. Sun, *Chem. Commun.*, 2013, **49**, 9134–9136.
33 J. Gitschier, B. Moffat, D. Reilly, W. I. Wood and W. J. Fairbrother, *Nat. Struct. Biol.*, 1998, **5**, 47–54.
34 Y. Xue, A. V. Davis, G. Balakrishnan, J. P. Stasser, B. M. Staehlin, P. Focia, T. G. Spiro, J. E. Penner-Hahn and T. V. O'Halloran, *Nat. Chem. Biol.*, 2008, **4**, 107–109.
35 L. Banci, I. Bertini, S. Ciofi-Baffoni, L. Gonnelli and X. C. Su, *J. Biol. Chem.*, 2003, **278**, 50506–50513.
36 Y. Fu, H. C. Tsui, K. E. Bruce, L. T. Sham, K. A. Higgins, J. P. Lisher, K. M. Kazmierczak, M. J. Maroney, C. E. Dann, M. E. Winkler and D. P. Giedroc, *Nat. Chem. Biol.*, 2013, **9**, 177–183.
37 S. J. Philips, M. Canalizo-Hernandez, I. Yildirim, G. C. Schatz, A. Mondragón and T. V. O'Halloran, *Science*, 2015, **349**, 877–881.
38 A. Changela, K. Chen, Y. Xue, J. Holschen, C. E. Outten, T. V. O'Halloran and A. Mondragón, *Science*, 2003, **301**, 1383–1387.
39 M. Meury, M. Knop and F. P. Seebeck, *Angew. Chem., Int. Ed.*, 2017, **56**, 8115–8119.
40 J. J. Braymer and D. P. Giedroc, *Curr. Opin. Chem. Biol.*, 2014, **19**, 59–66.
41 Z. Ma, F. E. Jacobsen and D. P. Giedroc, *Chem. Rev.*, 2009, **109**, 4644–4681.
42 H. B. Wang, X. M. Yang, M. J. Wang, M. L. Hu, X. H. Xu, A. X. Yan, Q. Hao, H. Y. Li and H. Sun, *Chem. Sci.*, 2020, **11**, 11714–11719.
43 R. A. Musrati, M. Kollarova, N. Mernik and D. Mikulasova, *Gen. Physiol. Biophys.*, 1998, **17**, 193–210.
44 S. J. Park, P. A. Cotter and R. P. Gunsalus, *J. Bacteriol.*, 1995, **177**, 6652–6656.
45 L. A. Fahien, E. H. Kmiotek, M. J. MacDonald, B. Fibich and M. Mandic, *J. Biol. Chem.*, 1988, **263**, 10687–10697.
46 T. R. Mullinax, J. N. Mock, A. J. McEvily and J. H. Harrison, *J. Biol. Chem.*, 1982, **257**, 13233–13239.
47 A. Bjørk, B. Dalhus, D. Mantzilas, V. G. H. Eijsink and R. Sirevåg, *J. Mol. Biol.*, 2003, **334**, 811–821.
48 J. K. Bell, H. P. Yennawar, S. K. Wright, J. R. Thompson, R. E. Viola and L. J. Banaszak, *J. Biol. Chem.*, 2001, **276**, 31156–31162.
49 K. Lee, H. S. Ban, R. Naik, Y. S. Hong, S. Son, B.-K. Kim, Y. Xia, K. B. Song, H.-S. Lee and M. Won, *Angew. Chem., Int. Ed.*, 2013, **52**, 10286–10289.
50 J. I. Boucher, J. R. Jacobowitz, B. C. Beckett, S. Classen and D. L. Theobald, *eLife*, 2014, **3**, e02304.
51 C. R. Goward and D. J. Nicholls, *Protein Sci.*, 1994, **3**, 1883–1888.
52 T. N. Minárik P, M. Kollárová and M. Antalík, *Gen. Physiol. Biophys.*, 2002, **21**, 257–265.
53 H. M. Wilks, K. W. Hart, R. Feeney, C. R. Dunn, H. Muirhead, W. N. Chia, D. A. Barstow, T. Atkinson, A. R. Clarke and J. J. Holbrook, *Science*, 1988, **242**, 1541–1544.
54 O. Dym, M. Mevarech and J. L. Sussman, *Science*, 1995, **267**, 1344–1346.
55 G. B. Kitto, P. M. Wassarman and N. O. Kaplan, *Proc. Natl. Acad. Sci. U. S. A.*, 1966, **56**, 578–585.
56 Y. Liu, A. Asnani, L. Zou, V. L. Bentley, M. Yu, Y. Wang, G. Dellaire, K. S. Sarkar, M. Dai, H. H. Chen, D. E. Sosnovik, J. T. Shin, D. A. Haber, J. N. Berman, W. Chao and R. T. Peterson, *Sci. Transl. Med.*, 2014, **6**, 266ra170.
57 J. Chen, S. Walter, A. L. Horwich and D. L. Smith, *Nat. Struct. Biol.*, 2001, **8**, 721–728.
58 Y. Yin and J. F. Kirsch, *Proc. Natl. Acad. Sci. U. S. A.*, 2007, **104**, 17353–17357.
59 C. S. Fermaintt and S. A. Wacker, *Essays Biochem.*, 2024, **68**, 147–160.
60 H. Wang, A. Yan, Z. Liu, X. Yang, Z. Xu, Y. Wang, R. Wang, M. Koohi-Moghadam, L. Hu, W. Xia, H. Tang, Y. Wang, H. Li and H. Sun, *PLoS Biol.*, 2019, **17**, e3000292.
61 L. Hu, T. Cheng, B. He, L. Li, Y. Wang, Y.-T. Lai, G. Jiang and H. Sun, *Angew. Chem., Int. Ed.*, 2013, **52**, 4916–4920.
62 D. M. Molina, R. Jafari, M. Ignatushchenko, T. Seki, E. A. Larsson, C. Dan, L. Sreekumar, Y. Cao and P. Nordlund, *Science*, 2013, **341**, 84–87.
63 R. Jafari, H. Almqvist, H. Axelsson, M. Ignatushchenko, T. Lundbäck, P. Nordlund and D. M. Molina, *Nat. Protoc.*, 2014, **9**, 2100.
64 M. D. Hall, D. G. Levitt and L. J. Banaszak, *J. Mol. Biol.*, 1992, **226**, 867–882.
65 M. D. Hall and L. J. Banaszak, *J. Mol. Biol.*, 1993, **232**, 213–222.
66 H. Wang, M. Wang, X. Yang, X. Xu, Q. Hao, A. Yan, M. Hu, R. Lobinski, H. Li and H. Sun, *Chem. Sci.*, 2019, **10**, 7193–7199.